Synchronization of cells with activator-inhibitor pathways through adaptive environment-mediated coupling

P. Guemkam Ghomsi
Complex systems and Theoretical Biology Group, Laboratory of Research on Advanced Materials and Nonlinear Science (LaRAMaNS), Department of Physics, Faculty of Science, University of Buea, P.O. Box 63 Buea-CAMEROON and Laboratoire de Mécanique, Department of Physics, Faculty of Science, University of Yaoundé I, P.O. Box 812, Yaoundé-Cameroon

F. M. Moukam Kakmeni*
Complex systems and Theoretical Biology Group, Laboratory of Research on Advanced Materials and Nonlinear Science (LaRAMaNS), Department of Physics, Faculty of Science, University of Buea, P.O. Box 63 Buea-CAMEROON and International Centre of Insect Physiology and Ecology, P.O. Box 30772-00100, Nairobi, Kenya

C. Tchawoua and T. C. Kofane
Laboratoire de Mécanique, Department of Physics, Faculty of Science, University of Yaoundé I, P.O. Box 812, Yaoundé-Cameroon
(Received 11 July 2015; published 24 November 2015)

In this paper, we report the synchronized dynamics of cells with activator-inhibitor pathways via an adaptive environment-mediated coupling scheme with feedbacks and control mechanisms. The adaptive character of the extracellular medium is modeled via its damping parameter as a physiological response aiming at annihilating the cellular differentiation existing between the chaotic biochemical pathways of the cells, in order to preserve homeostasis. We perform an investigation on the existence and stability of the synchronization manifold of the coupled system under the proposed coupling pattern. Both mathematical and computational tools suggest the accessibility of conducive prerequisites (conditions) for the emergence of a robust synchronous regime. The relevance of a phase-synchronized dynamics is appraised and several numerical indicators advocate for the prevalence of this fascinating phenomenon among the interacting cells in the phase space.

DOI: 10.1103/PhysRevE.92.052911 PACS number(s): 05.45.Xt, 87.17.Aa, 05.45.Gg

I. INTRODUCTION

The biochemical pathways involved in cellular metabolism can, depending on their parameter values, exhibit chaotic dynamics. This erratic behavior is more naturally and widely observed in many biological systems such as neural networks, cardiac pacemaker cells, animal gaits, metabolic networks [1–10], etc. The latter set includes arrays of cells with activator-inhibitor pathways [1,11,12]. In reality, there is nothing strange about it as it is well known that disorder is more likely than order. Incidentally, disorder happens more spontaneously while organization requires energy. Thus, energy and organization are closely related. Epitome of the latter concept is synchronization, which is a prerequisite for the coordinated collective behavior of cells. So, the synchronization dynamics of cells with activator-inhibitor pathways entails the existence of a potential energy of interaction among these biochemical systems, with suitable strength. This energy is brought in through several signaling schemes listed in the literature such as the electrical, chemical, environmental coupling types [1,11–13]. Depending on the nature of the interactions involved, these couplings can be of direct (or indirect), linear (or nonlinear) types. The literature is a great source of references reporting the ability of these couplings schemes to foster a synchronized dynamics in cellular ensembles [11–14].

However, it is well known that cells live in a common environment through which they interact indirectly with the diffusion and transport of chemical species across their membrane, and with the effects of the activation of receptors on their cellular membranes. Quite a sizable number of modeling studies of biochemical oscillators have been proposed in the literature [15–23]. For example, Guy Katriel investigated the environmental synchronization dynamics of the periodicities of a model for the pulsatile secretion of gonadotropin-releasing hormone from synchronized hypothalamic neurons. He could also explain the experimentally observed ability of thousand of cells to synchronize their periodic activity, crucial for the generation of macroscopic oscillations like circadian periodicities [24]. Cells perform numerous functions, and in order to carry out these tasks aiming at perpetuating life, cells need resources, most of which is obtained from their living environment. Competition for resources is therefore likely to occur among cells that interact through the same environment. Cell's fate, function, and phenotype is therefore affected by environmental cues. These interactions with the milieu create indirect ties between the cells. These connections among the biochemical pathways striving for resources shape biological niches. These interspecific interactions often limit the portion of their niche that they can actually use. Therefore, over time, the cells will make many complex adjustments to community living, evolving together and forging relationships that give the community its character and stability. Both competition and cooperation then play key roles as cooperation favors available resource partitioning, by this means reducing competition that can lead to extinction. Thus, in order to reach a balance, that is

*moukamkakmeni@gmail.com

homeostasis in the milieu, cells need to communicate. The state of each cell influences the state of the environment, and the environment in turns influences the cells. This phenomenon is called "coevolution," where different biochemical organisms evolve adjustments to one another over long periods of time. Biological systems have shown in many cases this ability to display a sufficiently rich variety of mechanical regulatory directives bequeathing them with the advantageous and useful skills of adaptation and learning [10].

The aim of this study is to explore the capacity of this indirect type of connection through an adaptive dynamic environment to foster a synchronized dynamics among cells with activator-inhibitor pathways as they diffuse in the environment their biochemical species referred to in this case as "synchronizing agents." In our analysis, we shall take into account the ability of these environmental connections to adapt to the biochemical changes occurring in the intercellular medium. This adaptation feature is crucial as we seek the synchronization dynamics of cells with activator-inhibitor pathways in their chaotic regime. Adaptive law have been widely used in the line of synchronization of chaotic systems ranging from chaotic oscillations, to chaotic circuits, to chaotic biological systems [25–28]. However, in this case, the adaptation law is brought in the system through environmental coupling. Their respective trajectories are known to continuously distribute along unstable directions in the phase space, due to their extreme sensitivity to initial conditions, inherently biasing them to flout synchronization. We find the synchronization dynamics of chaotic oscillators more appealing than that of periodic oscillators, especially with this weak form of coupling, interactions being indirect. To the best of our knowledge, this analysis has never been performed by other investigators and we deeply believe that its output will cast more light on the environmental processes sustaining high-quality cellular operations and determining the preservation of our existence.

This paper is organized as follows: in Sec. II, we present the coupled model portraying the adaptive environmental coupling of two cells with activator-inhibitor pathways. In Sec. III, we examine the existence and stability of the complete synchronous solution for our model based on the Lyapunov exponents. Subsequently, Sec. IV is devoted to the investigation on the appearance in the coupled system of a phase synchronized dynamics, whose importance has been proven by many researchers in biological networks. Section V concludes the work.

II. THE COUPLED MODEL

In the present study, we consider two chaotic cells with activator-inhibitor pathways, indirectly coupled through a common environment u with feedback and adaptive control mechanism, according to the following set of differential equations:

$$\begin{aligned}
\frac{dx_i}{dt} &= F(z_i) - kx_i,\\
\frac{dy_i}{dt} &= x_i - G(y_i,z_i),\\
\frac{dz_i}{dt} &= G(y_i,z_i) - qz_i - \epsilon_1\beta_i u,\\
\frac{du}{dt} &= -\kappa u - \epsilon_2\frac{(\beta_1 z_1 + \beta_2 z_2)}{2},\\
\frac{d\kappa}{dt} &= \alpha(\beta_1 z_1 + \beta_2 z_2)^2,
\end{aligned} \tag{1}$$

where $i = 1,2$, with $\beta_1 = -\beta_2 = 1$ and $0 < \alpha \ll 1$.

$F(z)$ and $G(y,z)$ are given by

$$F(z) = \frac{1}{1+z^4} \quad \text{and} \quad G(y,z) = \frac{Ty(1+y)(1+z)^2}{L+(1+y)^2(1+z)^2}.$$

They stand for the negative and positive feedback processes present in the sequence of biochemical reactions that internally contribute to maintain homeostasis in cellular functions by suppressing stochastic variations [29] and regulating activities in cellular processes that show periodic and complex dynamics. This is the case of glycolytic oscillations in cell-free extracts of yeast cells, peroxidase-oxidase reactions, calcium oscillations, etc. x_i, y_i, and z_i represent the normalized concentrations of the substrates and end-product of these cells' pathways. The parameters k and q are, respectively, the rate of degradation of the first substrate and the rate of degradation of the end product. T and L are related to the maximum velocity of the enzyme and the allosteric constant. u is a variable standing for the concentration of various biochemical species in the exterior of the cells, thereby globally determining the intrinsic dynamics of the environment, which is decaying with κ as its damping parameter. κ varies depending on the feedback from the systems, which in return enable the environment to sustain itself for extended periods of time. ϵ_1 is the strength of the feedback to the system and ϵ_2 is that to the environment. Here, we assume that the biochemical components of the cells that take part in the coupling are the end-products, as they diffuse through the environment with their respective normalized concentrations z_i. The nature of the feedback from and to the environment is prescribed by the values of β_1 and β_2. In the present case, the coupling is of difference type, that is $(\beta_1,\beta_2) = (1,-1)$. A similar model has been used by V. Resmi and G. Ambika [30] to couple Rössler and Lorenz systems through a common environment without adaptive feature. This coupling mechanism has the interesting property that the common environment does not alter the local chaotic dynamics of the systems as it attempts to synchronize them. In their synchronized regime, the systems preserve more or less the same phase space structure of the uncoupled system. Our idea consists in tuning the gain of a linear damping coefficient of the environmental coupling during the control procedure. We wish to update this gain with a proper adaptation law such that the proposed feedback control law can track and predetermine the optimal gain of the environmental controller.

Several references in the literature indicate that cells with activator-inhibitor pathways are complex systems capable of exhibiting complex dynamics ranging from simple limit cycle to chaotic behavior [11–13]. For their chaotic regime, the parameter values of their biochemical pathways carrying nonlinearities will be taken as: $q = 0.1$, $k = 0.003$, 10^6, and $T = 10$. It is noteworthy that cell signaling can occur in different forms. In the present work, we assume that

signal molecules released by cells can diffuse through the extracellular fluid to other cells. If those molecules are taken up by neighboring cells, destroyed by extracellular enzymes, or quickly removed from the extracellular fluid in some other way, their influence is restricted to cells in the immediate vicinity of the releasing cell. Such short-lived signals with local effects are called paracrine signals. They play crucial roles in the early development of the cell, coordinating the activities of clusters of cells. If a released signal molecule remains in the extracellular fluid, it may enter the organism's circulatory system and travel widely throughout the body. These longer-lived signal molecules, which may affect cells very distant from the releasing cell, are called hormones, and this type of intercellular communication is referred to as endocrine signaling. Both animals and plants use this signaling mechanism extensively.

It is worth mentioning that homeostasis is crucial for the survival of any living being. It refers to the maintenance of stable internal conditions in an organism living in a changing environment. The relevance of this importance lies on the fact that cells function best within a limited range of conditions. Therefore, for an active entity, temperature, blood sugar, acidity, and other conditions must be controlled. Failure to regulate these parameters may elicit detrimental functional disorder within the cellular ensemble pertaining to illness. To prevent this scenario, cells constantly convey their needs to the extracellular space in terms of organic resources by releasing some chemical signals, such as hormones across their plasma membrane in order to achieve their numerous tasks. Consequently, all cells regularly respond to their environment through steady feedback reports about their states and needs. These reactions are systematic processes that help our bodies to uphold their metabolic equilibrium states. Incidentally, it is the duty of their common dynamic extracellular medium to cater for their consistent demands by providing the required chemical resources. The aptitude of the environment to wisely make provisions for these cells sets the pace that is paramount to instate a harmonious cooperation among their pathways, thereby avoiding competition among them. Careful attention should be given to the fact that rivalry within the cellular milieu can be harmful for the smooth evolution and stability of the functional mechanisms involved in the developmental stages of the cells, aiming at maintaining homeostasis and perpetuating life.

Based on these facts, the steadiness of these cellular responses toward the environment in the course of time thereby enables us to assume in the present analysis that the strength of the feedbacks of the biochemical pathways to their living milieu, and vice versa, are constant throughout, and that only the extracellular medium adjusts its parameter values in terms of available resources in order to care for the biochemical systems which there live as a community. To achieve this, only the damping parameter κ of the dynamic environment will exhibit this adaptive feature, enabling the environment to constantly look for the optimal level in terms of availability and allocation of resources. Let us note that this optimal level also clearly depends on the cellular demand, that is the strength of the feedbacks ϵ_1 and ϵ_2. This is the reason why the subsequent study will be concerned with looking for the suitable values of ϵ_1 and ϵ_2 vital (necessary) to achieve this goal. Nonetheless, in other circumstances, these couplings (feedbacks) strengths could equally be considered to be adaptive and assumed to be influenced by hormones from other distant cells that bind to receptors on the target cell's membrane and trigger it to produce a needed chemical compound. However, this aspect of their operations shall not be taken into account in the present study. This may be the core of a later probe.

III. STABILITY OF THE COMPLETE SYNCHRONOUS SOLUTION

In coupled systems, synchronization refers to an adjustment of the time scales of their oscillations due to interaction between the oscillating processes. It is the most fundamental phenomenon that occurs in oscillating processes. At this stage, we wish to investigate the simultaneous existence and stability of a complete synchronous regime. In order to achieve this, we need to remind ourselves about the fact that the complete synchronized state lies on the synchronization manifold where the cells have exactly identical biochemical pathways, that is $x_1 = x_2$, $y_1 = y_2$, and $z_1 = z_2$.

A. Linear stability analysis of the coupled adaptive systems

Here, we investigate the stability of the synchronous state of two systems coupled via the scheme of Eq. (1). Let ξ_1, ξ_2, v, and η be the deviations from the synchronized state of the two coupled systems, the environment, and the damping parameter, respectively, which are all dynamic. Their dynamics is governed by the linearized equations obtained from Eq. (1), which in matrix form can be written as

$$\begin{aligned}
\frac{dX_1}{dt} &= f(X_1) + \epsilon_1\gamma\beta_1 u,\\
\frac{dX_2}{dt} &= f(X_2) + \epsilon_1\gamma\beta_2 u,\\
\frac{du}{dt} &= -\kappa u - \frac{\epsilon_2}{2}\gamma^T(\beta_1 X_1 + \beta_2 X_2),\\
\frac{d\kappa}{dt} &= \alpha[\gamma^T(\beta_1 X_1 + \beta_2 X_2)]^2,
\end{aligned} \tag{2}$$

where X_1, X_2, u, and κ have dimension 3, 3, 1, and 1, respectively. γ is a column matrix (3×1) with elements zero or one and it decides the components of X_i that take part in the coupling. We then get

$$\begin{aligned}
\frac{d\xi_1}{dt} &= f'(X_1)\xi_1 + \epsilon_1\gamma\beta_1 v,\\
\frac{d\xi_2}{dt} &= f'(X_2)\xi_2 + \epsilon_1\gamma\beta_2 v,\\
\frac{dv}{dt} &= -\kappa v - \frac{\epsilon_2}{2}\gamma^T(\beta_1\xi_1 + \beta_2\xi_2) - v\eta,\\
\frac{d\eta}{dt} &= 2\alpha[\gamma^T(\beta_1 X_1 + \beta_2 X_2)]\gamma^T(\beta_1\xi_1 + \beta_2\xi_2).
\end{aligned} \tag{3}$$

For a completely synchronized regime, that is $X_1 = X_2$, Eq. (3) can be reduced by defining

$$\xi_0 = \beta_1\xi_1 + \beta_2\xi_2, \tag{4}$$

then Eq. (3) reads

$$\begin{aligned}\frac{d\xi_0}{dt} &= f'(X_1)\xi_0 + \epsilon_1(\beta_1^2+\beta_2^2)\gamma v,\\ \frac{dv}{dt} &= -\kappa v - v\eta - \frac{\epsilon_2}{2}\gamma^T\xi_0,\\ \frac{d\eta}{dt} &= 2\alpha\gamma^T(\beta_1 X_1 + \beta_2 X_2)\gamma^T\xi_0.\end{aligned} \tag{5}$$

The fixed point (0,0,0) of Eq. (5) corresponding to the synchronized state will be stable if all the Lyapunov exponents derived from Eq. (3) are negative. A significant development can be made if we assume that the time average values of $f'(X_1)$ and $f'(X_2)$ are approximately the same and can be replaced by an effective constant value μ [30]. Similarly, $\beta_1 X_1 + \beta_2 X_2$ can be replaced by its time average constant value ω. In this approximation, we treat ξ_1 and ξ_2 as scalars. This type of approximation has been employed in Ref. [36], and it was observed that it describes the overall features of the phase diagram judiciously well. Thus, using ξ_0 defined by Eq. (4), Eq. (3) can be written as

$$\frac{d\xi_0}{dt} = \mu\xi_0 + 2\epsilon_1 v, \tag{6}$$

$$\frac{dv}{dt} = -\kappa v - v\eta - \frac{\epsilon_2}{2}\xi_0, \tag{7}$$

$$\frac{d\eta}{dt} = 2\alpha\omega\xi_0, \tag{8}$$

where we have $\beta_1^2 + \beta_2^2 = 2$.

Differentiating Eq. (6) with respect to time and eliminating v from Eq. (6) and Eq. (7), we derive an equation for ξ_0 given as

$$\ddot{\xi_0} = (\mu - \kappa - \eta)\dot{\xi_0} + [\mu(\kappa+\eta) - \epsilon_1\epsilon_2]\xi_0. \tag{9}$$

After differentiating again Eq. (9) with respect to time and discarding all the deviation terms of order two (namely $\xi_0\dot{\xi_0}$, ξ_0^2, $\ddot{\xi_0}\eta$, and $\eta\dot{\xi_0}$), we find the equation

$$\frac{d^3\xi_0}{dt^3} + (\kappa-\mu)\ddot{\xi_0} + [\epsilon_1\epsilon_2 + \alpha\omega^2 - \mu\kappa]\dot{\xi_0} - \mu\alpha\omega^2\xi_0 = 0. \tag{10}$$

Assuming a solution of the form $\xi_0 = Ae^{mt}$, we obtain the eigenvalue equation

$$m^3 + (\kappa-\mu)m^2 + [\epsilon_1\epsilon_2 + \alpha\omega^2 - \mu\kappa]m - \mu\alpha\omega^2 = 0. \tag{11}$$

The parameter values of μ and ω can be obtained numerically from the time series of the coupled system as the temporal averaging values of the functions $\dot{z_i}$ and $\beta_1 z_1 + \beta_2 z_2$ over a long period of time (because the coupling scheme is implemented via the third variable, that is the end-product concentration) when weak perturbations are performed on the synchronization manifold. In this regard, the values of $\mu \approx 0.00612611845$ and $\omega \approx 1.0$ are found. For the sake of simplicity, we will choose the value $\kappa = 1.0$ in order to ensure that the value of the damping parameter be greater than all of the optimal values of κ observed numerically (depending on the initial conditions) and necessary to obtain a synchronous solution, when the coupling strength is suitable to instate a synchronized regime in the coupled system. We take $\alpha = 3.5001 \times 10^{-9}$.

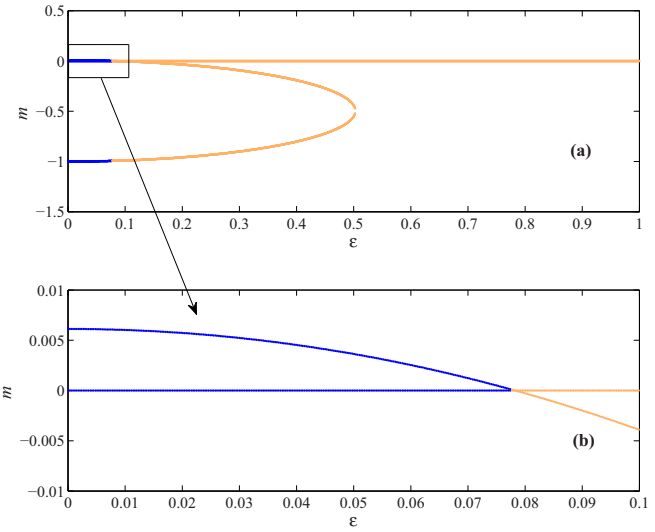

FIG. 1. (Color online) The spectrum of eigenvalues as a function of ϵ: (a) Eigenvalue spectrum for which the synchronized state is unstable, $\epsilon \leqslant 0.0771$ in dark line (blue online); Eigenvalue spectrum for which the synchronized state is stable, $\epsilon > 0.0771$ in gray line (orange online). (b) Zoom of the small box in (a) as an evidence of the existence of at least one eigenvalue that exceeds zero, thereby yielding an unstable synchronization manifold when $\epsilon \leqslant 0.0771$. The parameter values are $\mu = 0.00612611845$, $\omega = 1.0$, $\kappa = 1.0$, and $\alpha = 3.5001 \times 10^{-9}$.

Based on the above considerations and on the assumption that $\epsilon_1 = \epsilon_2 = \epsilon$, we solve Eq. (11) for the eigenvalues of our system making use of the dichotomy scheme, for different values of ϵ. The solutions obtained are depicted on Fig. 1(a) and it is observed that all the eigenvalues m (orange online) are always less than or equal to zero provided that the coupling strength $\epsilon > 0.0771$. This indicates that for this range of values of the coupling the synchronous state is stable. This is in close agreement with the previous result observed numerically on Fig. 2 through the plot of the evolution of the Lyapunov spectrum as a function of ϵ where a similar trend was noticed for $\epsilon > 0.07$. To ascertain this fact, an enlargement of the region $\epsilon < 0.0771$ indicated by the rectangular box in Fig. 1(a) is shown in Fig. 1(b). This figure clearly suggests that for $\epsilon \leqslant 0.0771$, there exists at least one eigenvalue that visibly exceeds zero and will contribute to the generation of an unstable synchronization manifold. As inference, we can say that both numerical and analytical tools advocate for the suitable interval of value of $\epsilon > 0.0771$, for which the synchronized regime attained through our adaptive feedback-control scheme of two environmentally coupled cells with activator-inhibitor pathways is stable.

B. Numerical simulation of the Lyapunov Spectrum

Our study of the stability of this manifold will be based on the calculation of the Lyapunov spectrum of the coupled system. Lyapunov exponents are known to assess the fast exponential divergence of two trajectories of the same

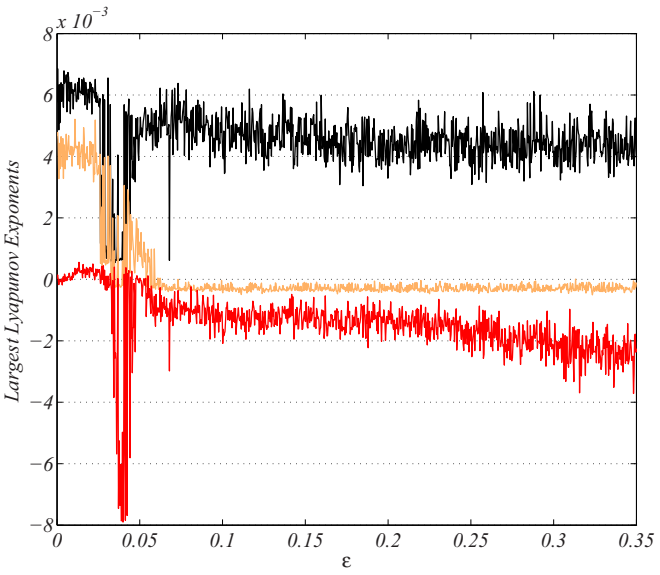

FIG. 2. (Color online) The three largest Lyapunov exponents of the coupled system as a function of the coupling strength ϵ. The parameter values are $q = 0.1$, $k = 0.003$, $L = 10^6$, $T = 10$.

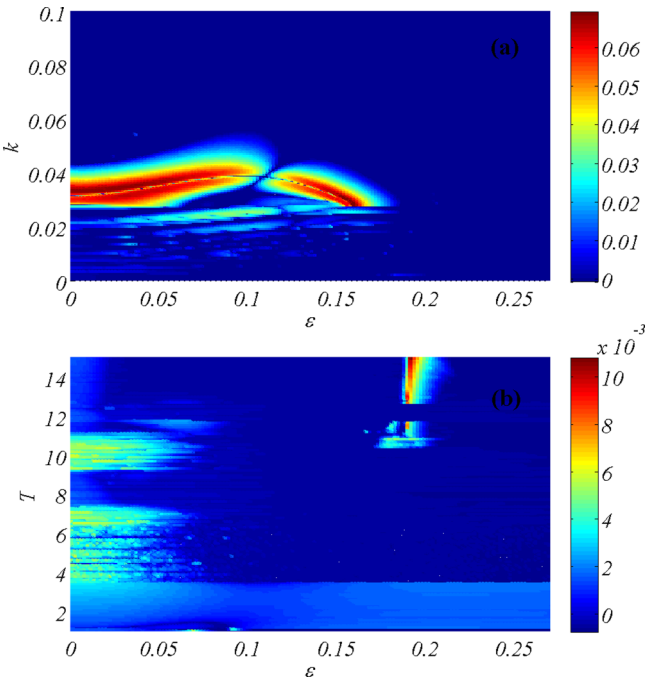

FIG. 3. (Color online) The Lyapunov diagrams of the coupled system Eq. (1), defined by the second-largest Lyapunov exponent of the spectrum, showing domains of stability of the synchronization manifold as function of the coupling strength ϵ and (a) the rate of degradation of the first substrate k and (b) the maximum velocity of the enzyme T. The other parameters are fixed as $L = 10^6$ and $q = 0.1$.

dynamical system, which started from almost indistinguishably close initial conditions in the phase space and with the course of time. In the actual case study, when the coupled systems are completely synchronized, they act as one unique entity on the synchronization manifold, thereby causing the dimension of the coupled cells to settle from 8 to 4. In the event where perturbations are produced on the manifold in directions transverse to it, that dimension unfolds again in phase space and grows above 4, leaving the system unsynchronized. A survey of how these perturbations grow in the phase space over a long period of time can be perceived through the calculation of the whole spectrum of Lyapunov exponents corresponding to the coupled system for a given value of the coupling strength. The technique for the obtention of this spectrum is described in Ref. [35]. It produces 8 Lyapunov exponents. First and foremost, the largest of them, λ_1, is an indicator of whether there is a chaotic dynamics on at least one of the coupled systems. In our case, because of the chaotic dynamics of the cells, λ_1 is always strictly positive for all the values of ϵ. Second, and extremely important, the second largest exponent λ_2 of our coupled system detects whenever a fully stable synchronized regime is instated among the cells by the coupling. This occurs when λ_2 becomes strictly negative. Finally, and not the least, the third Lyapunov exponent λ_3 provides information about the presence of a phase synchronized dynamics among the cells.

Before closing this discussion, we support the previous relevant comments made on the ability of this feedback-control adaptive environmental coupling to preserve the local intrinsic chaotic behavior of cells while synchronizing them, by plotting the three largest Lyapunov exponents of our 8-dimensional coupled system as a function of the environmental coupling scheme. This is presented in Fig. 2 where it is observed that the largest Lyapunov exponent is always strictly positive irrespective of the value of ϵ, showing that the global dynamics of the coupled system is always chaotic. Also, we observe that the third largest Lyapunov exponent definitely becomes negative when $\epsilon > 0.066$, indicating the onset of phase synchronization. In addition, when $\epsilon > 0.07$, the second largest Lyapunov exponent becomes steadily negative, indicating in its turns the onset of complete chaotic synchronization for the coupled cells. These results are in agreement with our previous observations.

Therefore, in order to enquire about the existence and stability of the synchronous solution, we will rely on the observations made on the evolution of λ_2 as we vary the strength of the coupling among the cells. Figure 3(a) depicts the domains of stability of the synchronized state in the (ϵ,k) parameter space based on λ_2. It is observed that cells find it easy to synchronize for most of the couple of values (ϵ,k) of the coupling strength and the rate of degradation of the first substrate, except mainly when $(\epsilon,k) \in [0.028,0.055] \times [0,0.18]$; and for some few isolated points spread in the lower region of the parameter space. Figure 3(b) shows the same analysis performed in the (ϵ,T) parameter space, where we see that the domain of stability is still large. But, the stable synchronized state is not accessible when the maximum velocity of the enzyme is such that $T \in [1,3.8]$, and mostly when $(\epsilon,T) \in [0,0.065] \times ([1,7.5] \cup [9.1,11.2])$.

Evidence of these observations are portrayed in Fig. 4, where we plot both the time series superpositions of the cells and their phase portrait correlations for two different values of ϵ. The parameter values are still those for the chaotic dynamics of the pathways. When $\epsilon = 0$, Fig. 4(a) shows that the cells are not synchronized and their phase portrait

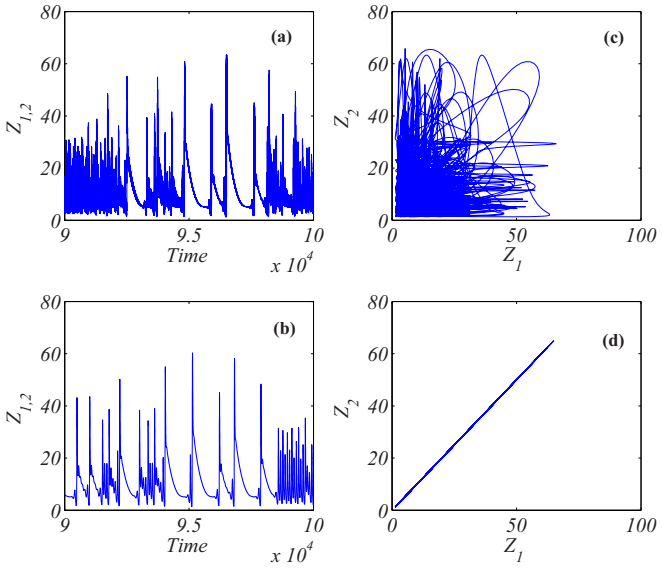

FIG. 4. (Color online) Complete synchronization in two indirectly coupled cells with activator-inhibitor pathways coupled through an adaptive environment with feedback control mechanism. Figures (a) $\epsilon = 0$, no synchronization, and (b) $\epsilon = 0.15$, synchronization, are the plots of the superposition of the time series of the two coupled cells. Figures (c) $\epsilon = 0$, no synchronization, and (d) $\epsilon = 0.15$, are the correlation graphs for different values of the coupling. For a suitable coupling strength, a complete synchronized dynamics is obtained.

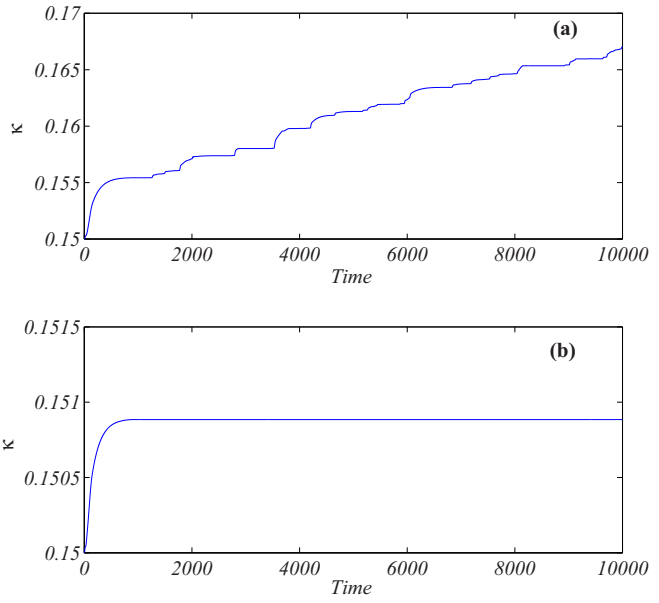

FIG. 5. (Color online) Time series of the damping parameter of the environment κ for (a) $\epsilon = 0$ and (b) $\epsilon = 0.15$.

correlation graph shows that they are uncorrelated as seen on Fig. 4(c). However, when $\epsilon = 0.15$, Figs. 4(b) and 4(d) show that the cells have their biochemical pathways perfectly synchronized and correlated via their end-product normalized concentration.

It then becomes obvious that the proposed adaptive environmental coupling scheme is capable of producing a robust synchrony among the coupled cells with activator-inhibitor pathways. The adaptation and learning skills of this coupling involve dynamical processes that tend to reinforce themselves through long-term repeated experience of encoding, assimilating, and decoding of information produced both endogenously and exogenously. Figure 5 portrays the adaptive character of this indirect coupling scheme with feedback control, where it is observed that for the value of the coupling $\epsilon = 0$, the damping parameter κ of the environment continuously grows with time, indicating that the coupled system cannot reach a stable synchronized dynamics. But for a suitable value of the coupling, κ increases and rapidly attains a constant value, corresponding to its optimal value when synchronization is established among the cells.

IV. PHASE SYNCHRONIZATION

When seeking procedures to assess to degree of synchronization between two oscillators, sufficient attention must be given to their respective "stages" of oscillations, that is their positions inside the specified cycle of oscillations; namely the beginning, the first quarter, the middle, the third quarter, the end, etc. The quantity responsible of characterizing the stage of oscillations of each oscillator at any instant of time is called the phase of that oscillator [$\phi(t)$]. For harmonic oscillations, the phase is a linear function of time, while for more complex dynamics such as quasiharmonic and chaotic oscillations, it has a more complex shape. Accordingly, the concept of phase is intimately associated with the phenomenon of synchronization. Phase therefore represents a convenient tool for the detection of whether two oscillators are synchronized or not. Specifically, considering the phase difference between oscillators, if the phase difference happens to be a constant or to slightly swing around a constant, this would typically suggest that the oscillators are 1:1 synchronized. In this case, there is the appearance of frequency locking mechanisms due to the effect of suitable coupling scheme and strength, forcing the oscillators to vibrate "in phase." Alternatively, if the phase difference grows in time, there is no 1:1 synchronization.

As well as in nature it is hard to find two exactly identical systems, complete synchronization is more challenging to find compared to phase synchronization. Mindful of this fact, phase synchronization therefore occurs more naturally in coupled biological systems. It is the weakest form of synchronization and is usually obtained when the strength of interactions is low. As the coupling strengths become large, more ordered levels of synchronization regimes appear such as lag synchronization, followed by the strongest synchronized dynamics: the complete synchronization [11]. The intermittency in the phase synchronized dynamics usually takes place at the values of the coupling strength where transitions between these different types of synchronized regimes are obtained. This intermittency is characterized by intervals of loss of synchronization disconnecting epochs of synchronization.

In coupled dynamical systems, several indicators of the presence of a phase synchronized dynamics can be used such as the average phase difference between two systems, the stroboscopic poincaré maps, the Lyapunov exponents, the phase-space diffusion and correlation parameters, namely the

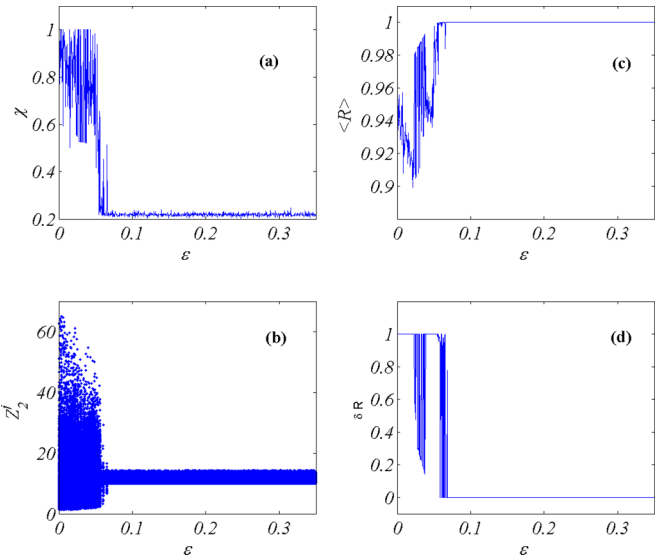

FIG. 6. (Color online) Onset of phase synchronization in two indirectly coupled cells with activator-inhibitor pathways coupled through an adaptive environment with feedback control mechanism. (a) Occupation of the conditional observations with respect to the attractor, χ. (b) End-product Normalized concentration z_2^j of the second cell when the first cell makes the jth crossing with the section $z = 10$, for $\dot{z} > 0$. (c) Mean value of the Kuramoto parameter $\langle R \rangle$. (d) The Kuramoto amplitude δR, as a function of the coupling strength $\epsilon_1 = \epsilon_2 = \epsilon$, detecting the emergence of phase synchronization in the coupled biochemical system. The parameter values are $q = 0.1$, $k = 0.003$, $L = 10^6$, $T = 10$.

Kuramoto parameter, to name just a few. First, it is noteworthy that a strong evidence of the existence of phase synchronization in coupled chaotic oscillators is the localization of conditional sets obtained from the observations of the position of one cell's trajectory at the time another cell makes any physical event [31]. This concept is an extension of the approach of localized map by Pereira *et al.* [32] who demonstrated that localized sets can be constructed while in phase synchronization by means of any physical observation. In the present study, we define our physical event based on the poincaré section of the attractor of the first cell through the plane defined by $z = 10$, with the constraint that $\dot{z} > 0$. In this manner, based on the repeated realizations in the phase space of the defined event by the trajectory of the first cell, a stroboscopic map is derived for the second cell through observations of its positions at the times the event takes place. A set of points is therefore constructed in phase space for the second cell for a given value of the coupling strength. For the sake of simplicity, we assume that $\epsilon_1 = \epsilon_2 = \epsilon$ as in the preceding analysis.

To have a clear picture of when phase synchronization might appear between the two coupled chaotic cells, we show in Fig. 6(a) the plot of the quantity:

$$\chi = \frac{\max\left(z_2^j\right) - \min\left(z_2^j\right)}{\max[z_2(t)] - \min[z_2(t)]}, \tag{12}$$

where z_2^j represents the value of z_2 at the instant the trajectory of the first cell makes the jth event. Thus χ is related to how broad the conditional observations spread over the whole attractor [33]. Figure 6(b) depicts the captured values of z_2^j on the attractor of the second cell in phase space at the times the event occurs, for different values of ϵ. It appears from both figures that when $\epsilon > 0.066$, phase synchronization takes place, as the conditional observations obtained for the second cell when the first one makes the event always produce a localized set of points. Alongside this analysis, we carry out a temporal survey of the data using the parameter

$$R = \frac{\sqrt{\left(\sum_{i=1}^{2} \sin(\phi_i)\right)^2 + \left[\sum_{i=1}^{2} \cos(\phi_i)\right]^2}}{2}, \tag{13}$$

defined by Kuramoto in 1984 as a rigorous quantity for the assessment of mutual phase entrainment and synchronization among coupled phase oscillators [34]. ϕ_i stands for the phase of the ith cell. For a given set of parameters, we compute the temporal average $\langle R \rangle$ of R and its amplitude $\delta R = \max_t(R) - \min_t(R)$. For full (complete) synchronization to be established, we consider that the following conditions must be fulfilled:

$\langle R \rangle$ is strictly greater than $\langle R \rangle_{\text{threshold}} = 0.98$ and that

$\delta R < \delta R_{\text{threshold}} = 0.001$

Both $\langle R \rangle_{\text{threshold}}$ and $\delta R_{\text{threshold}}$ have values chosen arbitrarily. Figures 6(c) and 6(d) show the evolutions of $\langle R \rangle$ and δR, respectively, obtained over a long period of time, as the environmental coupling ϵ varies. As previously indicated in the case of the generation of conditional sets, it is observed that when $\epsilon > 0.066$, phase synchronization takes place, immediately followed by the emergence of a high quality full synchronization.

As illustrative evidences of the above remarks, we present, respectively, in Figs. 7(a) and 7(c) the set of points obtained in dark dots (blue online) from the second cell's attractor through the Poincaré section of the first cell's attractor at the times the defined event takes place, and the time series of the phase difference between the cells, when $\epsilon = 0$. It is observed that the set of points are not localized and the time series of the phase difference show divergence as it is not bounded. The calculations indeed show in Fig. 7(c) that the phase difference goes up to 4×10^4. For a larger value of the environmental coupling, namely $\epsilon = 0.15$, the set of points become localized as seen on Fig. 7(b). Hence, the corresponding phase difference between the biochemical pathways on Fig. 7(d) becomes perfectly zero due to the fact that they are completely synchronized for the given value of the environmental coupling.

We finalize our study on the appearance of phase synchronization in the coupled system by investigating in the parameter spaces (ϵ,k) and (ϵ,T) suitable requirements for the emergence of this synchronized regime, based on the mean value of the Kuramoto parameter. On both parameter space diagrams, the domains of phase synchronization are depicted in black (blue). From Fig. 8(a), it appears that a phase synchronized regime is almost always present in the coupled system as soon as $\epsilon > 0.066$, except in general for $k \in [0.0028, 0.029]$ where the synchronized dynamics is more or less reluctant to appear for a large range of values of ϵ. The exception made is that the domain of existence of phase synchronization in the parameter space (ϵ,k) is very large. Thus, the coupled cells are more inclined to synchronize their biochemical pathways for a wide range of

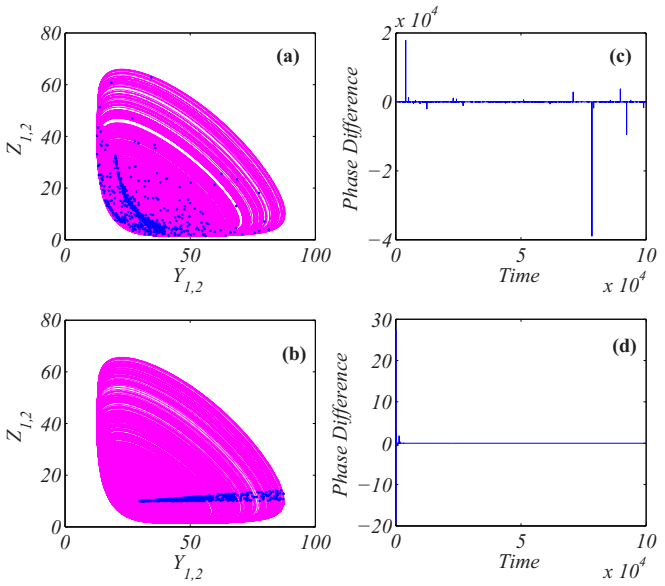

FIG. 7. (Color online) Onset of phase synchronization in two indirectly coupled cells with activator-inhibitor pathways coupled through an adaptive environment with feedback control mechanism. Figures (a) $\epsilon = 0$ and (b) $\epsilon = 0.15$ are the plots of the attractor of the first cell in gray lines (pink online) and the stroboscopic projection of the attractor of the second cell in dark dots (blue online) on the cross section of the first cell, for different values of the coupling strength (the points are localized as the coupling increases, indicating the onset of phase synchronization in the system). Figures (c) $\epsilon = 0$ and (d) $\epsilon = 0.15$ are time series of the phase difference of the two coupled cells for different values of the coupling. As the coupling increases, the phase difference is bounded, confirming the onset of phase synchronization in the biochemical system. The parameter values are the same as described in the caption of of Fig. (6).

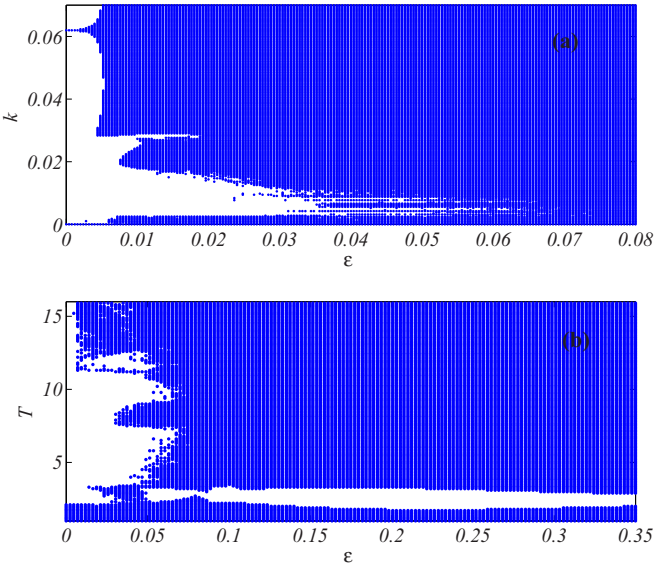

FIG. 8. (Color online) The Kuramoto diagrams of the coupled system Eq. (1), based on the mean value of the Kuramoto parameter, showing phase synchronization regions in black (blue) and regions of unsynchronized dynamics white (white) as a function of the coupling strength ϵ and (a) the rate of degradation of the first substrate k and (b) the maximum velocity of the enzyme T. The other parameter being fixed as $L = 10^6$ and $q = 0.1$.

parameter points (ϵ,k). Figure 8(b) equally shows that in the parameter space (ϵ,T) there is a narrow band of points for which the maximum velocity of the enzyme $T \in [1.7,3.4]$ and the coupling strength $\epsilon \in [0,0.07233]$, where the coupled system defies synchronization. But exception made of these regions is that a wide part of the parameter space (ϵ,T) is greatly in favor of the emergence of a phase synchronized dynamics. The above analysis performed on the concept of phase synchronization in coupled systems is particularly important since it determines immensely the spatiotemporal organization of coupled biological systems and the efficiency with which information is transferred from one cell to another.

V. DISCUSSIONS AND CONCLUSION

The foregone outcomes derived from our model provide good reenactments about the internal processes pertaining in high-quality physiological activities occurring in living beings, as observed through many practical inspections. It is worth mentioning that our model, which is inspired by several preceding works addressing a broad area of valid problems encompassing indirectly coupled biological and complex systems, and sometimes unveiling prominent chaotic activities with time-delay schemes, is supported by key data collected in culture experiments [24,37–39]. Specifically, some data have enabled the authors in [24,37] to draw a comprehensive set of valuable assumptions on an analogous model of gonadotropin-releasing hormone (GnRH) from synchronized hypothalamic nerve cells. The analysis of the dependence of the equilibrium levels of α subunits, of Ca^{2+} and cAMP on G proteins on the basis of experimental data has been implemented. This study showed the adaptive character of these elements. The simulations of many heterogeneous neurons have revealed the robustness of their synchronization mediated by a common pool of diffusible GnRH, which there plays the role of synchronizing agent in the midst of the nerve cells. Likewise, Ref. [40] proposes a similar approach to model biochemical signal transduction systems based on a defined aggregate objective function that likely accounts for the evolutionarily optimized efficiency in signal transmission in the extracellular medium. Starting from the ground that concentration adjustment in the cellular milieu exists to maintain effective signal transmission, the author showed that her model is self-organizing, as perturbations in proteins concentrations or changes in extracellular signaling automatically lead to adaptation. After systematic perturbations in the protein concentrations, she observed the responses and reaction times (that is the delays) of 27 molecular species involved in a set of 23 chemical reactions seemingly driving the optimization. Hypothesizing that an efficient signal transmission would maximize the responses of the molecular species to the input, she defined the objective function so as to minimize the delay and maximize the response. This procedure had pertinence in explaining the adaptation scenarios.

Also, Ref. [10] clearly reports some experimental observations obtained about the functional responses of the environmental properties, with relevance in the instatement

of a harmonious development in the cellular milieu. Therein, it is clearly given account about the fact that the animal body has evolved over a long period of time, and specialization (that is the richness in the diversity of species) has increased. With pertinence in each specie, cells are found to be sophisticated machines finely tuned to carry out a precise role within the body. Such specialization of cells is possible only when extracellular conditions are kept within narrow limits. Temperature, pH, the concentration of glucose and oxygen, and many other factors must be kept constant for cells to function efficiently and interact properly with one another. Homeostasis, which is essential for life, may then be defined as the dynamic constancy of the internal environment. The term *dynamic* is used because conditions are never absolutely constant, but fluctuate continuously within narrow limits. However, in the present analysis we ideally assume through our model their constancy for the sake of simplicity, that is the constancy of the damping parameter κ of the environment whenever complete synchronization is achieved, as shown in Fig. 5(b). This optimal value of κ helps stabilizing the environmental conditions and concomitantly annihilates the cellular differentiation. In order to maintain homeostasis, vertebrates possess several sensors that are able to measure each environmental condition. They constantly monitor the extracellular conditions and relay this information, usually (via nerve signals) to an *integrating center*, which contains the *set point*, that is the proper value for that condition (see Chap. 58, "Maintaining the internal environment," in Ref. [10]).

The *integrating center* is often a particular region of the brain or spinal cord, but it can also sometimes be cells of the endocrine glands. It receives messages from several sensors, weighing the relative strengths of each sensor inputs, and then determines whether the value of the condition is deviating from the set point. When a deviation in a condition occurs, which is referred to in this case as a *stimulus*, the *integrating center* sends a message to increase or decrease the activity of particular effectors, which are generally muscles or glands that can change the value of the condition in question, back toward the set-point value: This is referred to as the *response*. The effectiveness of this mechanism relies on a type of control system known as *negative (or reverse) feedback loop*. For example, it is well known that if the body (or blood) temperature (which fundamentally determines the fate of biochemical reactions in the intra- and intercellular medium, cells being osmoregulator) exceeds 37 °C (98.6°F), sensors in a part of the brain detect this deviation. Acting via an *integrating center* also located in the brain (namely the hypothalamus), these sensors stimulate effectors, including sweat glands, that lower the temperature, thereby protecting the set points of the body against deviations. Conversely, if the temperature happens to go below 37 °C, a different set of responses is generated, such as shivering and the constriction of blood vessels in the skin, which help to raise the body temperature and correct the initial challenge to homeostasis. These regulations are in the reverse (or negative) directions, and are therefore referred to as negative feedback loops crucial for the maintenance of homeostasis, and that ultimately cause the effectors to be turned off. In this way, constancy in environmental conditions is maintained, thereby enhancing a coordinated collective agreement among the environmentally connected biochemical pathways of the cells. Therefore, the regulation of body temperature, blood glucose, and other environmental parameters in the cellular milieu has as an end objective the stabilization of environmental patterns aiming at ensuring optimal conditions for the emergence of a harmonious cellular development.

Subsequent to this perusal of experimental observations, and all together with our theoretical results, it appears evident that our proposed model reliably depicts a fairly faithful description of the importance of the steadiness in an optimal level (set point), of the parameter values of the environment, herein portrayed by its damping parameter κ, and achieved via adaptive feedback control mechanisms. Its regulatory feature has as an end result the promotion of a robust synchronized dynamics among the cells with activator-inhibitor pathways, which can efficiently communicate via stable environmentally relayed signallings.

As we summarize the work done so far, it is important to recall that cells with activator-inhibitor pathways are biochemical systems capable of parading an extremely rich variety of complex dynamical behaviors such as fixed points and periodic and chaotic regimes. In lattices, they are also known to display, depending on their population size, interesting features of spatiotemporal organization, when directly interacting under steady coupling conditions [1,11–13]. In the above inquiry, we have investigated their synchronized dynamics assuming that they interact indirectly through a dynamic environment with adaptive feedback control mechanism, aiming at promoting a cooperative pattern between the biochemical pathways of the chaotic cells, by stabilizing in the phase space their trajectories that lean toward disseminating themselves along unsteady directions, setting them to flout synchronization. Though a weak form of coupling, this coupling mode has proven itself capable of engendering robust synchrony among cells with activator-inhibitor pathways. The stability analysis of the synchronized state has been carried out in this framework and the numerical simulations suggest the existence of many suitable conditions that favor the emergence of this highly desirable collaborative arrangement among the cells.

ACKNOWLEDGMENTS

F.M.M.K. would like to express his gratitude to the Deutscher Akademischer Austausch Dienst (DAAD), Germany, for financial support under the Research Grant section ST 32 Africa, ICN: 91584646, and also the International Centre of Insect Physiology and Ecology (ICIPE), for financial and material supports.

[1] S. Sinha and R. Ramaswamy, in *Chaos in Biological Systems*, edited by H. Degn, A. V. Holden, and L. F. Olsen (Plenum Press, New York, 1987).

[2] D. Hebb, *The Organization of Behavior* (New York, Wiley, 1949),

[3] S. H. Strogatz and I. Stewat, Sic. Am. **269**, 102 (1993).

[4] D. Helbing and B. A. Huberman, Nature **396**, 738 (1998).
[5] A. T. Winfree, *The Geometry of Biology Time*, 2nd ed. (Springer, New York, 2001).
[6] I. Z. Kiss, Y. Zhai, and J. L. Hudson, Science **296**, 1676 (2002).
[7] A. T. Winfree, Science **298**, 2336 (2002).
[8] S. Nadis, Nature **421**, 780 (2003).
[9] S. H. Strogatz, *Sync: The Emerging Science of Spontaneous Order* (Hyperion, New York, 2003).
[10] P. Raven, G. Johnson, K. Mason, J. Losos, and S. Singer, *Biology*, 10th ed. (McGraw-Hill Education, New York, 2013).
[11] S. Rajesh, S. Sinha, and S. Sinha, Phys. Rev. E **75**, 011906 (2007).
[12] P. Guemkam Ghomsi, F. M. Moukam Kakmeni, T. C. Kofane, and C. Tchawoua, Phys. Lett. A **378**, 2813 (2014).
[13] C. Suguna and S. Sinha, Physica A **346**, 154-164 (2005).
[14] J. Garcia-Ojalvo, M. B. Elowitz, and S. H. Strogatz, Proc. Natl. Acad. Sci. USA **101**, 10955 (2004).
[15] J. R. Collier, N. A. M. Monk, P. K. Maini, and J. H. Lewis, J. Theor. Biol. **183**, 429 (1996).
[16] J. Keener and J. Sneyd, *Mathematical Physiology* (Springer-Verlag, New York, 1998).
[17] J. Monod, J. Wyman, and J. P. Changeaux, J. Mol. Biol. **12**, 88 (1965).
[18] G. von Dassow, E. Meir, E. M. Munro, and G. M. Odell, Nature **406**, 188 (2000).
[19] M. B. Miller and B. L. Bassler, Annu. Rev. Microbiol. **55**, 165 (2001).
[20] M. Freeman and J. B. Gurdon, Annu. Rev. Cell Dev. Biol. **18**, 515 (2002).
[21] J. Wolf and R. Heinrich, BioSystems **43**, 1 (1997).
[22] A. Goldbeter, *Biochemical Oscillations and Cellular Rhythms. The Molecular Bases of Periodic and Chaotic Behavior* (Cambridge University Press, Cambridge, 1996).
[23] O. Decroly and A. Goldbeter, Proc. Natl. Acad. Sci. USA **79**, 6917 (1982).
[24] G. Katriel, Physica D **237**, 2933 (2008).
[25] S. A. Lazzouni, S. Bowong, F. M. Moukam Kakmeni, and B. Cherki, Commun. Nonlin. Sci. Numer. Simul. **12**, 568 (2007).
[26] F. M. Moukam Kakmeni and S. Bowong, Int. J. Bifurcat. Chaos **17**, 3259 (2007).
[27] S. Bowong, F. M. Moukam Kakmeni, and C. Tchawoua, Phys. Rev. E **70**, 066217 (2004).
[28] F. M. Moukam Kakmeni, S. Bowong, C. Tchawoua, and E. Kaptouom, Phys. Lett. A **322**, 263 (2004).
[29] H. H. McAdams and A. P. Arkin, Proc. Natl. Acad. Sci. USA **94**, 814 (1997).
[30] V. Resmi, G. Ambika, and R. E. Amritkar, Phys. Rev. E **81**, 046216 (2010).
[31] T. Pereira, M. S. Baptista, and J. Kurths, Phys. Lett. A **362**, 159 (2007).
[32] T. Pereira, M. S. Baptista, and J. Kurths, Phys. Rev. E **75**, 026216 (2007).
[33] F. M. Moukam Kakmeni and M. S. Baptista, Pramana **70**, 1063 (2008).
[34] Andreas Bohn and Jordi Garcia-Ojalvo, J. Theor. Biol. **250**, 37 (2008).
[35] A. Wolf, J. B. Swift, H. L. Swinney, and J. A. Vastano, Physica D **16**, 285 (1985).
[36] G. Ambika and R. E. Amritkar, Phys. Rev. E **79**, 056206 (2009).
[37] A. Khadra and Y. X. Li, Biophys. J. **91**, 74 (2006).
[38] D. Ghosh and T. Banerjee, Phys. Rev. E **90**, 062908 (2014).
[39] T. Banerjee and D. Biswas, Nonlin. Dyn. **73**, 2025 (2013).
[40] G. Scheler, F1000Research **2**, 116 (2013).